https://doi.org/10.5194/hess-2020-407
Preprint. Discussion started: 9 September 2020

Hydrology and Earth System Sciences Discussions
Open Access

The added value of brightness temperature assimilation for the SMAP Level-4 surface and root-zone soil moisture analysis over mainland China

Jianxiu Qiu[1,2], Jianzhi Dong[3], Wade T. Crow[3], Xiaohu Zhang[4,5], Rolf H. Reichle[6], Gabrielle J. M. De Lannoy[7]

[1]Guangdong Provincial Key Laboratory of Urbanization and Geo-simulation, School of Geography and Planning, Sun Yat-sen University, Guangzhou, 510275, China

[2]Southern Laboratory of Ocean Science and Engineering (Guangdong, Zhuhai), Zhuhai, 519000, China

[3]USDA ARS Hydrology and Remote Sensing Laboratory, Beltsville, MD 20705, USA

[4]National Engineering and Technology Center for Information Agriculture, Nanjing Agricultural University, Nanjing, China

[5]Jiangsu Key Laboratory for Information Agriculture, Nanjing Agricultural University, Nanjing, China

[6]Global Modeling and Assimilation Office, NASA Goddard Space Flight Center, Greenbelt, MD, USA

[7]Department of Earth and Environmental Sciences, KU Leuven, Heverlee, Belgium

Correspondence to: Jianxiu Qiu (qiujianxiu@mail.sysu.edu.cn)

Abstract. The Soil Moisture Active Passive (SMAP) Level-4 Surface Soil Moisture and Root-Zone Soil Moisture (L4) product provides global estimates of surface soil moisture (SSM) and root-zone soil moisture (RZSM) via the assimilation of SMAP brightness temperature (Tb) observations into the Catchment Land Surface Model (CLSM). Here, using in-situ measurements from 2474 sites in mainland China, we evaluate the performance of soil moisture estimates from L4 and from a baseline "open-loop" (OL) simulation of CLSM without Tb assimilation. Using random forest regression, the efficiency of the L4 data assimilation (DA) system (i.e., the performance improvement in L4 relative to OL) is attributed to 8 control factors related to the land surface modelling (LSM) and radiative transfer modeling (RTM) components of the L4 system. Results show that 77% of the 2287 9-km EASE grid cells in mainland China that contain at least one ground station exhibit an increase in the Spearman rank correlation skill (R) with in-situ measurements for L4 SSM compared to that of OL, with an average R increase of approximately 14% (ΔR = 0.056). RZSM skill is improved for about the same percentage of 9-km EASE grid cells, but the average R increase for RZSM is only 7% (ΔR = 0.034). Results further show that the SSM DA efficiency is most strongly related to the error in Tb observation space, followed by the error in precipitation forcing and microwave soil roughness. For RZSM DA efficiency, the three dominant control factors remain the same, although the importance of soil roughness exceeds that of the Tb error. For the skill of the L4 and OL estimates themselves, the top control factors are the precipitation error and the SSM-RZSM coupling strength error (in descending order of factor importance for R_{OL}), both of which are related to the LSM component of the L4 system. Finally, we find that the L4 system can effectively filter out errors in precipitation. Therefore, future development of the L4 system should focus on improving the characterization of the SSM-RZSM coupling strength.

Keywords. SMAP Level 4, soil moisture, data assimilation, attribute analysis, random forest regression

1 Introduction

Soil moisture modulates water and energy feedbacks between the land surface and the lower atmosphere by determining the partitioning of incoming net radiation into latent and sensible heat (Seneviratne et al., 2010, 2013). High-quality, global-scale soil moisture products have become increasingly available in recent years (Gruber et al., 2020). In particular, the L-band NASA Soil Moisture Active Passive (SMAP) satellite mission (Entekhabi et al., 2010; Piepmeier et al., 2017) has significantly improved the skill of available, global-scale soil moisture products. However, the SMAP observations contain temporal data gaps and are only representative of conditions within the top 5 cm of the vertical soil moisture column. To address these limitations, the SMAP Level-4 Surface and Root-Zone Soil Moisture (L4) algorithm assimilates SMAP brightness temperature (Tb) observations into the NASA Catchment Land Surface Model (CLSM) to derive an analysis of surface (0–5 cm) and root-zone (0–100 cm) soil moisture estimates with global, 3-hourly coverage (Reichle et al., 2017a; Reichle et al., 2017b; Reichle et al., 2019).

However, the performance of a land data assimilation (DA) system is sensitive to its parameterization and requires careful assessment. For instance, Reichle et al. (2008) demonstrate that DA based on incorrect assumptions of modeling and observation errors can degrade soil moisture estimates, compared with the case of not performing any DA. Theoretically, the optimality of DA can be evaluated using so-called innovations, or observations-minus-forecast residuals; however, an investigation of the innovations alone is often insufficient to determine if the soil moisture analysis is optimal (Crow and Van Loon, 2006).

Recently, Dong et al. (2019a) proposed a novel statistical framework for evaluating the performance of a soil moisture DA system. Specifically, they demonstrated that the relative skill of surface soil moisture (SSM) estimates acquired with and without DA can be estimated using the ratio of their correlations with just one noisy but independent ancillary remote sensing product. This approach was applied to the SMAP L4 system using ASCAT soil moisture retrievals. Their results show that the added value of SMAP DA is closely related to both rain gauge and vegetation density. However, due to the limited availability of independent root-zone soil moisture (RZSM) products for performing statistical error estimation, this method is only applicable for SSM estimates.

Relative to SSM, the efficiency of assimilating land surface observations to improve RZSM is complicated by model structural error that affects the ability of the DA to update unobserved model states. For instance, Kumar et al. (2009) identified the surface–root zone coupling strength, which is the result of a model-dependent representation of processes related to the partitioning of rainfall into infiltration, runoff, and evaporation components, as an important factor for determining RZSM improvement associated with the assimilation of SSM retrievals. Their synthetic experiments suggest that – faced with unknown true subsurface physics – overestimating the surface–root zone coupling in the land model is a more robust strategy for obtaining skill improvements in the root zone than under-estimating the coupling. Likewise, Chen et al. (2011) suggested that their Soil and Water Assessment Tool significantly under-predicts the magnitude of vertical soil water coupling in the Cobb Creek Watershed in southwestern Oklahoma, USA, and this lack of coupling impedes the ability of DA to effectively update deep-layer soil moisture, groundwater flow and surface runoff. In the context of the present paper, the evaluation of L4 RZSM estimates has been limited to relatively few SMAP core validation and sparse network sites (Reichle et al., 2017a; Reichle et al., 2017b; Reichle et al., 2019). With such limited sample sizes, the RZSM skill of the L4 product at the global scale remains uncertain.

The primary objective of this study is to determine the DA efficiency, i.e., performance improvement in DA results relative to the open-loop (OL) baseline of the L4 product, as a function of a variety of system aspects, including errors in CLSM forcing (e.g., precipitation), errors in key CLSM parameters (e.g., relating to vegetation), mean errors in CLSM structure (e.g., surface and root-zone coupling), and errors in the radiative transfer modeling (RTM) that links the modeled soil moisture and temperature estimates to the observed Tb.

To this end, we first evaluate the performance of L4 SSM and RZSM estimates using a very large number (n = 2474) of soil moisture profile measurement sites (generally acquired at sub-surface depths between 10 and 50 cm) within mainland China. Next, the in-situ measurements are used to assess the DA efficiency of the L4 system, which is defined as the skill difference between the L4 estimates and model-only estimates derived without SMAP Tb assimilation. Additionally, we apply a machine-learning technique to quantify by how much various control factors drive the spatial variations in the efficiency of the L4 system. In this way, we seek to prioritize future enhancements to the L4 system.

2 Data and Methods

This section briefly describes the SMAP L4 soil moisture product (Section 2.1), the extensive network of in-situ soil moisture observations over mainland China (Section 2.2) and the ancillary data sources and metrics used in the skill assessment (Sections 2.3 and 2.4). Next, we introduce the double instrumental variable (IVd) method employed to determine the errors in control factors that cannot be determined using ground observations (Section 2.5). Finally, we describe the random forest (RF) regression method used to identify the main factor(s) (out of the 8 control factors from both CLSM and RTM aspects) that affect the spatial variations in SMAP L4 DA efficiency and L4 performance (Section 2.6).

2.1 SMAP L4 soil moisture product

The SMAP L4 soil moisture product (version 4; Reichle et al., 2019) is generated by assimilating the SMAP L1C Radiometer half-orbit 36 km EASE-Grid brightness temperature (Tb) observations (Version 4 SPL1CTB; Chan et al., 2016) into the CLSM. The SMAP Tb observations are assimilated at 3-h intervals using a spatially distributed, 24-member ensemble Kalman filter (Reichle et al. 2017b). The surface meteorological forcing data are from the global Goddard Earth Observing System (GEOS) Forward Processing atmospheric analysis (Lucchesi, 2013), with precipitation corrected using the daily, 0.5-degree, gauge-based Climate Prediction Center Unified (CPCU) product (Xie et al. 2007). The L4 product provides global, 9-km, 3-hourly surface (0–5 cm) and root-zone (0–100 cm) soil moisture estimates along with related land surface fields and analysis diagnostics. For the present study, we aggregated all soil moisture estimates to daily-average (00:00 to 23:59 UTC) data. A baseline, model-only, ensemble CLSM simulation without the assimilation of SMAP Tb observations (but using the same perturbations as in the L4 system) is referred to as the "open-loop" (OL) run.

The SMAP L4 assimilation system includes a zero-order "tau-omega" forward RTM (De Lannoy et al., 2013) that converts SSM and surface soil temperature into L-band brightness temperature estimates. Selected parameters of the L4 RTM, including microwave soil roughness parameters, a vegetation structure parameter, and the microwave scattering albedo, were calibrated using multi-angular L-band brightness temperature observations from the Soil Moisture Ocean Salinity (SMOS) mission (De Lannoy et al., 2014). The L4 RTM parameterizes microwave soil roughness as a function of SSM (De Lannoy et al., 2013, their equation B1). Here, we used this parameterization to compute the 2017-2018 time-averaged microwave soil roughness estimates as one potential indicator of DA efficiency (Section 2.3). The necessary parameters were obtained from L4 "Land-Model-Constants" output Collection (last access: 8 July 2020; DOI: https://doi.org/10.5067/KGLC3UH4TMAQ; Reichle et al., 2018a). The L4 "Analysis-Update-Data" output Collection includes RTM predictions of Tb and the assimilated SMAP Tb observations (last access: 8 July 2020; DOI: https://doi.org/10.5067/60HB8VIP2T8W; Reichle et al., 2018b).

https://doi.org/10.5194/hess-2020-407
Preprint. Discussion started: 9 September 2020

Hydrology and Earth System Sciences
Discussions

To avoid the impact of seasonality, we performed our analysis using anomaly time series, derived by subtracting a seasonally-varying (daily) climatology from each raw time series. The climatology of a given time series was obtained by sampling the mean value of all soil moisture estimates that fall within a 31-day moving window centered on a particular day-of-year. Moreover, L4 estimates of land latent heat flux (LE), land sensible heat flux (SH) and the climatological LAI inputs to CLSM and the RTM, were obtained from the L4 "Geophysical-Data" output Collection (last access: 6 April 2020; DOI: https://doi.org/10.5067/KPJNN2GI1DQR; Reichle et al., 2018c). These datasets were also used to compute control factors to explain spatial variations in the DA efficiency of the L4 system (Section 2.3).

2.2 Soil moisture validation data

In-situ soil moisture measurements during 2017 and 2018 were collected from a national network of Chinese Automatic Soil Moisture Observation Stations (CASMOS) maintained by the Chinese Meteorological Administration (CMA). In total, soil moisture measurements from 2474 separate stations arrayed across mainland China, and covering different land use types, were collected. At each CASMOS site, frequency domain reflectometry-based instruments were used to record hourly volumetric soil moisture content within the following vertical depth ranges: 0–10, 10–20, 20–30, 30–40, and 40–50 cm below the surface. These hourly estimates (at multiple depths) were then aggregated into daily values and linearly averaged (vertically) to produce 0-10 cm (SSM) and 0-50 cm (RZSM) in situ soil moisture measurements – which were subsequently used to validate the L4 and OL SSM (0-5 cm) and RZSM (0-100 cm) estimates. Note that Spearman correlation rather than Pearson correlation is used for L4 and OL validation, in order to avoid impact of outliers in the time series and prior assumptions about soil moisture distributions.

Ground observations falling within the same 9-km EASE grid were averaged for comparisons against the collocated 9-km L4 and OL soil moisture estimates. A total of 2287 individual 9-km EASE grid cells within mainland China are included in the analysis. Among them, 92.35% of grid cells contain one in-situ site, 7.26% contain two sites, 7 grid cells contain three sites, and the remaining two grid cells contain four and five sites respectively.

2.3 Explanatory data products

As discussed above, our hypothesis is that the efficiency of the SMAP L4 system will be sensitive to the ability of the ensemble-based L4 analysis in filtering errors that exist in the OL (that is, CLSM), in the model forecast Tb (that is, the RTM), and in the SMAP Tb observations. We therefore considered two separate categories of factors that potentially control spatial variations in DA efficiency. The factors are summarized in Table 1.

The first category represents a range of factors known to affect the skill of soil moisture estimates derived from LSM (in this case, CLSM). The five control factors in this category are: i) the error in precipitation forcing, ii) the error in (input) LAI, iii) the error in (output) LE, iv) the magnitude of mean error in CLSM SSM-RZSM coupling strength, and v) the presence of vertical variability in soil properties (defined as the difference in clay fraction across the vertical soil profile). Note that such variability represents a potential source of error because CLSM assumes that soil texture and the associated soil parameters are vertically homogeneous within the soil column, with the exception of some

https://doi.org/10.5194/hess-2020-407
Preprint. Discussion started: 9 September 2020

surface-layer moisture transport parameters. The soil texture information is from Harmonized World Soil Database (HWSD) v1.2.

The second category contains three factors that affect radiative transfer modeling (RTM) and therefore DA updates. These include: i) estimates of the joint error in SMAP Tb observations and RTM Tb simulations, ii) the magnitude of microwave soil roughness, and iii) the magnitude of LAI (as a proxy for the vegetation optical depth at microwave frequencies, which modulates the sensitivity of the observed Tb to SSM conditions).

The control factors take a variety of forms. Some factors are based on estimates of the errors fed into the L4 system as (e.g., the error in CLSM rainfall forcing data). Other factors consist of the magnitude of the variable itself (e.g., the vertical variability of clay fraction). Note that LAI is used in both ways: LAI error is used to predict OL performance (because LAI is an important input into CLSM) while mean LAI is used to explain DA performance (because increased LAI is associated with decreased soil moisture information content in microwave observations).

Note that the LAI used in the L4 system is a climatology derived from satellite observations of the Normalized Difference Vegetation Index. Therefore, to indicate the magnitude by which each grid cell's LAI typically deviates from its long-term climatology, we use the temporal standard deviation of anomaly time series of the benchmark LAI (from SPOT VGT product) as a measure of the error in the LAI used in L4. Owing to the lack of reference Tb observations at similar satellite overpass times and locations, Tb errors are gauged using the time series standard deviation of the observation-minus-forecast (O-F) Tb residuals, which indicate the typical misfit between the model forecast Tb and the (rescaled) SMAP Tb observations. This metric measures the total error in Tb observation space. The exact data sets and the metrics utilized for evaluating these 8 control factors are summarized in Table 1.

https://doi.org/10.5194/hess-2020-407
Preprint. Discussion started: 9 September 2020

Table 1 Benchmark data sets and metrics used for evaluating control factors of SMAP L4

Factor category	Control factor	Dataset/Benchmark	Temporal resolution	Spatial resolution	Data range	Metrics
LSM	Precipitation error	Rain gauge (CGDPA)	daily	0.25 °	2017-2018	Spearman's rank correlation *R*
	SSM-RZSM coupling strength error	CASMOS	daily	NA	2017-2018	ΔCP (see Section 2.4)
	Vertical variability of clay fraction	HWSD	NA	9 km	NA	Difference in clay fraction between topsoil (0-30 cm) and root-zone (0-100 cm) layers
	SMAP L4 LAI error	SPOT LAI	10 d	1 km	2017-2018	Temporal standard deviation of SPOT VGT LAI anomaly
	LE error	FLUXCOM	daily	(1/120) °	2017-2018	IVd-based *R*
RTM	Tb error	SMAP L4	daily	9 km	2017-2018	Temporal standard deviation of O-F Tb residuals
	Microwave soil roughness	SMAP L4	daily	9 km	2017-2018	Temporal average based on De Lannoy et al. (2013)
	Annual mean LAI	MODIS/Geoland-based product	daily	9 km	2017-2018	Climatological mean

2.3.1 Gauge-based precipitation gridded product

Errors in the GEOS precipitation data used to force the CLSM within the SMAP L4 system were estimated via Spearman's rank correlation with available rain-gauge observations. These network observations are based on an analysis of ~2400 rain gauge stations distributed unevenly over mainland China. Recently, the China Gauge-based Daily Precipitation Analysis (CGDPA) with a spatial resolution of 0.25 °×0.25 °based on this network was constructed and has been made operational over mainland China. CGDPA uses a modified interpolation method of climatology-based optimal interpolation (OI) with topographic correction proposed by Xie et al. (2007). In this process, daily precipitation climatology over mainland China is optimized and is rebuilt using the 30-year average precipitation observations from ~2400 gauges of the period 1971–2000 (Shen et al., 2010). CGDPA is shown to have smaller bias and root mean square error than the CPCU product used in L4, which is based on fewer than 400 gauge sites over mainland China (Shen et al., 2015).

2.3.2 FLUXCOM LE estimates

The FLUXCOM ensemble of global land-atmosphere energy fluxes was used to evaluate the error of the L4 LE estimates. This ensemble merges energy flux measurements from FLUXNET eddy covariance towers with remote sensing and meteorological data based on a machine learning method to estimate global gridded net radiation, latent and sensible heat and their related uncertainties (Jung et al., 2019). The resulting FLUXCOM database has a 0.0833 ° spatial resolution when applied using MODIS remote sensing data. The monthly energy flux data of all ensemble members, as well as the ensemble estimates from the FLUXCOM initiative, are freely available (CC4.0 BY license) from the Data Portal (http://fluxcom.org/), while the daily- and 8-day FLUXCOM products are available upon request from dataset provider Martin Jung. To calculate the LE error, we've collected the daily, high spatial resolution FLUXCOM product and extracted the estimates where in-situ soil moisture sites located.

2.3.3 SPOT VGT LAI

The data set used as a benchmark for assessing leaf area index (LAI) errors present in the SMAP L4 analysis was derived from SPOT/VEGETATION and PROBA-V LAI products (version 2) that are generated every 10 days at spatial resolution of 1 km. The SPOT LAI version 2 product capitalizes on the development and validation of already existing products: CYCLOPES version 3.1 and MODIS collection 5 and the use of neural networks (Baret et al., 2013; Verger et al., 2008). The version 2 products are derived from top of canopy daily (S1-TOC) reflectances instead of normalized top of canopy 30-day composited reflectances as in the version 1. Compared to version 1, the compositing step is performed at the biophysical variable level instead of reflectance level. This ensures reduced sensitivity to missing observations and avoids the need for a BRDF model.

2.3.4 HWSD soil texture

The HWSD attribute database (v1.2) is a 30 arc-second raster database with 15773 different soil-mapping units. It provides information on the standardized soil parameters for topsoil (0–30cm) and subsoil (30-100 cm) separately. In this study, we use the difference of clay fractions between topsoil (0-30cm) and the aggregated 0-100cm layer to measure the vertical clay fraction variation at each 9-km grid cell.

2.4 Vertical coupling metric

The RZSM time series generally show decreased temporal dynamics relative to SSM. As a result, overestimated SSM-RZSM coupling tends to spuriously increase the (correlation-based) similarity of SSM and RZSM time series, and thereby, overestimate RZSM temporal variability. Therefore, analogous to Kling-Gupta efficiency (Gupta et al., 2009), we defined the SSM-RZSM coupling strength (CP) as:

$$\mathrm{CP} = 1\text{-}\sqrt{(R\text{-}1)^2 + (\alpha\text{-}1)^2} \tag{1}$$

where R is the Spearman's rank correlation between SSM and RZSM, and α is the ratio of temporal standard deviation of SSM to that of RZSM. A CP value of one represents the extreme case where RZSM is identical to SSM, i.e., a strongly coupled case. Likewise, a CP of zero represents the opposing case of completely uncoupled time series. Cases with negative CP do not exist.

Observed CP (CP_{obs}) was based on comparisons between 0-10 cm "surface" estimates and 0-50 cm "root-zone" in situ observations and used as a benchmark. In contrast, SMAP L4 CP estimates (CP_{OL}) was based on the comparison of 0-5 cm "surface" estimates and 0-100 cm "root-zone" estimates. Therefore, the surface versus root-zone storage contrast in the observation time series is less than that of the L4 estimates. This will likely cause the observed correlation between surface and root-zone time series to be systematically higher than the analogous vertical correlation calculation for L4 estimates. However, this bias is partially corrected for by the second term in Eq. (1) – since the observed α ratio will, by the same token, tend to be smaller (i.e. closer to one) than α sampled from the L4 analysis. Such ability to compensate for vertical depth differences is a key reason we apply CP, rather than *simple correlation*, as a vertical coupling strength metric. Nevertheless, it should be noted that our main interest here lies in describing spatial variations in (CP_{OL} - CP_{obs}) and care should be taken when interpreting raw (CP_{OL} - CP_{obs}) differences as an *absolute* measure of L4 vertical coupling bias.

2.5 Double instrumental variable (IVd) method

The benchmark data set of FLUXCOM LE described above contains error that is (likely) of a similar order of magnitude as the L4 LE dataset it is applied to evaluate. Therefore, in an attempt to correct for the impact of this error, the LE error used here as a control factor is obtained via a double instrumental variable (IVd; Dong et al., 2019b) analysis approach that minimizes the spurious impact of random errors in benchmark data sets. As shown in Dong et al. (2019b), for the evaluation of two time series with auto-correlation in both of them, IVd is more robust than single instrumental variable based algorithm, therefore we apply IVd to evaluate the LE error.

https://doi.org/10.5194/hess-2020-407
Preprint. Discussion started: 9 September 2020

IVd is a modified version of triple collocation (TC) analysis. In TC analysis (McColl et al., 2014), geophysical variables obtained from three independent sources (x, y and z) are assumed to be linearly related to the true signal P as:

$$x = \alpha_x P + B_x + \varepsilon_x \tag{2}$$

where the α_x is a scaling factor; B_x is a temporal constant bias and ε_x is zero-mean random error.

As opposed to the TC method, IVd uses only two independent products (x, y) to characterize geophysical data product errors. This method introduces two instrumental variables (I and J, i.e., $I_t = \alpha_x P_{t\text{-}1} + B_x + \varepsilon_{xt\text{-}1}$, $J_t = \alpha_y P_{t\text{-}1} + B_y + \varepsilon_{yt\text{-}1}$), which are based on the lag-1 (day) time series (at day t) of x and y, respectively. Therefore, assuming that the errors of two independent products are serially white, the covariance between instrumental variables and products can be written as follows:

$$C_{Ix} = \alpha_x^2 L_{PP} \tag{3}$$

$$C_{Jy} = \alpha_y^2 L_{PP} \tag{4}$$

where C represents the covariance of the subscript products. For instance, C_{Ix} represents the covariance of x and its instrumental variable I. Variable L_{PP} is the lag-1 auto-covariance of the true signal. Combining Eqs. (3) and (4), the scaling ratio s_{ivd} of the two products x and y can be written as:

$$s_{ivd} = \sqrt{\frac{C_{Ix}}{C_{Jy}}} \tag{5}$$

Based on Eq. (5), their correlation with truth can be estimated as:

$$R_{Px}^2 = \frac{C_{xy} s_{ivd}}{C_{xx}} \tag{6}$$

$$R_{Py}^2 = \frac{C_{xy}}{C_{yy} s_{ivd}} \tag{7}$$

In this way, the error in the L4 LE (measured by IVd-based correlation with truth) can be estimated robustly using the FLUXCOM LE product described in Section 2.3.2.

https://doi.org/10.5194/hess-2020-407
Preprint. Discussion started: 9 September 2020

2.6 Random forest regression

A random forest (RF) regression approach was used to rank and quantify the importance of the 8 control factors introduced above (Table 1) for describing spatial patterns in DA efficiency for both SSM and RZSM estimates. The RF method is a supervised learning algorithm based on an averaged ensemble of decision trees (Breiman, 2001). Unlike linear regression approaches, RF can capture non-linear interactions between the features and the target. In addition, the normalization (or scaling) of data is not necessary in RF application. Another advantage of the RF algorithm is that it can readily measure the relative importance of each feature on the estimates, which makes it highly suitable for an attribution analysis. Therefore, based on the output of RF, key control factors determining the efficiency of SMAP DA were evaluated and ranked. The RF estimates are based on a 10-fold cross-validation approach.

3 Results

3.1 Validation of SMAP L4 and OL estimates of SSM and RZSM anomalies

Figure 1 maps validation results (i.e., anomaly Spearman's rank correlation with in-situ observations, R) for SMAP L4 and associated OL soil moisture estimates. The skill patterns for OL and L4 are, in general, quite spatially consistent. Both are characterized by an increasing trend of SSM estimation skill moving from northwest to southeast China (Fig. 1a and 1b). In relative terms, the L4 product surpasses the baseline OL's SSM skill within 77% of the 2287 9-km EASE grid cells containing ground observations – with a mean R increase of ΔR = 0.056 [-] and mean relative improvement versus R_{OL} of 14%.

Similar spatial patterns are observed for RZSM skill. As with SSM, generally higher consistency with in-situ RZSM measurements is found in southeast China relative to northern China. However, relative to SSM, the added value of SMAP data assimilation (i.e. L4) is reduced for RZSM and the mean relative R improvement falls to 7% (ΔR = 0.034 [-]) (compare Fig. 1e and 1f). This is not surprising since assimilated SMAP Tbs are primarily sensitive to soil moisture conditions in the surface (0-5 cm) layer.

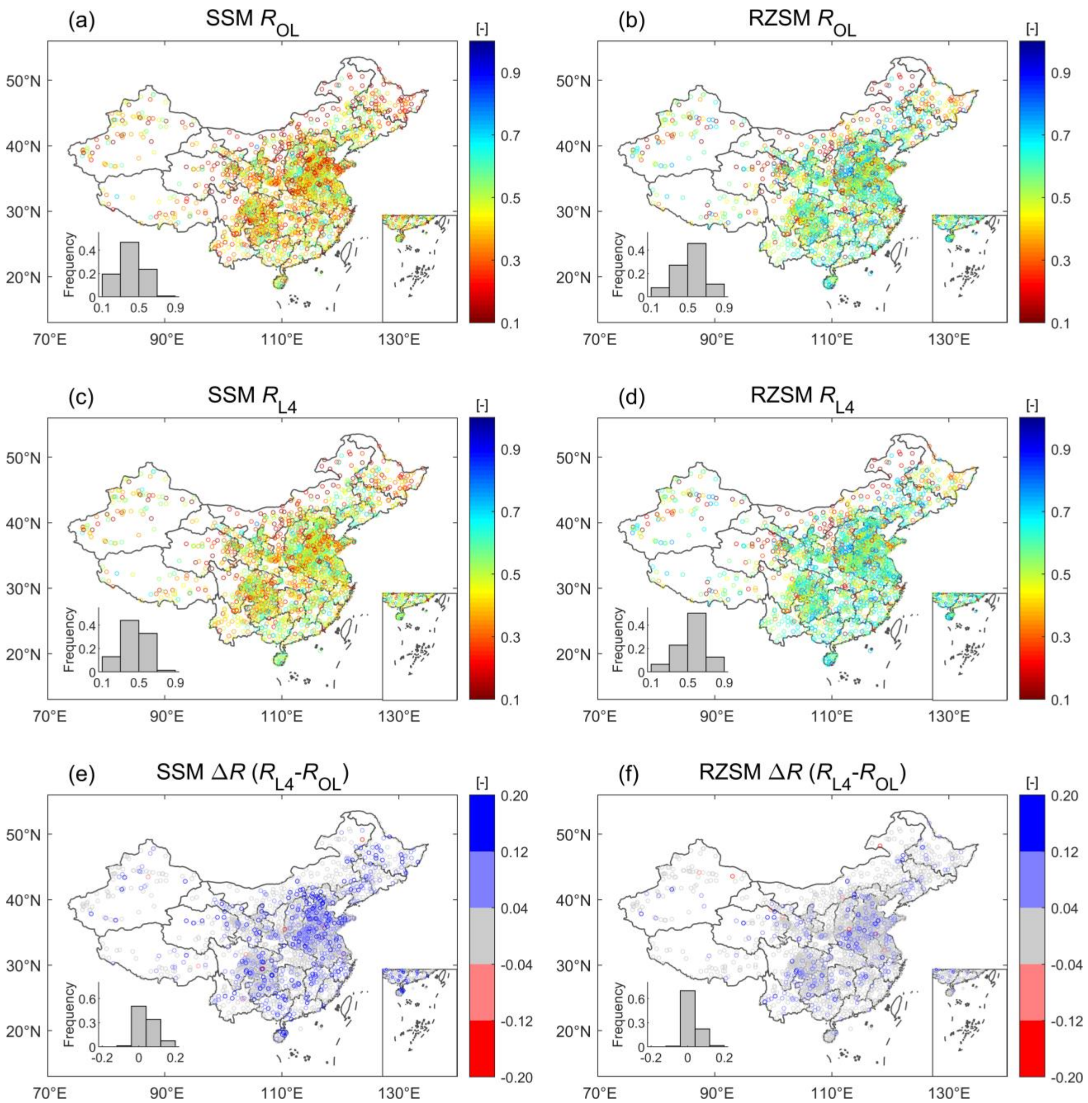

Figure 1: OL (a, b) and L4 (c, d) skills (*R* values) for SSM (left column) and RZSM (right column). DA efficiency ($\Delta R = R_{L4} - R_{OL}$) for (e) SSM and (f) RZSM. Blue (red) colors in (e) and (f) indicate grid cells where L4 estimates are better (worse) than OL. Non-significant differences (based on a 1000-member bootstrapping analysis) are colored grey. The lower left inset in each subplot indicates the frequency of binned *R*-values across all 9-km EASE grid cells containing ground observations.

3.2 Spatial distribution of potential factors controlling SMAP L4 DA performance

As described in Section 2.3, we selected 8 control factors that potentially influence the skill of SMAP L4 soil moisture estimates. Using the attribution analysis described in Section 2.6, these factors will be used to explain the spatial

https://doi.org/10.5194/hess-2020-407
Preprint. Discussion started: 9 September 2020

variations in skill and DA efficiency seen in Fig. 1. As a first step, this section examines the spatial patterns inherent in the 8 control factors. Errors in the CLSM precipitation forcing are relatively higher in northern and northwestern areas of China (Fig. 2a), where the gauge density is generally more sparse than southern China. Among the factors representing CLSM structural errors, a pre-dominantly negative bias is observed in SSM-RZSM coupling strength generally across China (i.e., lower CP_{OL} compared to CP_{obs}), while a very small number of grid cells show a positive coupling strength bias in eastern China (dark green dots in Fig. 2b). This is expected since at the coarse resolution, the model's vertical coupling strength should be much less than at any single point. In addition, this may be partly attributed to the layer depths differences, since CLSM represents surface and root-zone depths of 0-5 cm and 0-100 cm, whereas the corresponding in-situ observations represent the 0-10 cm and 0-50 cm layers, and it can be expected that CP_{OL} should thus be smaller than CP_{obs}. In addition, the vertical variability of the clay fraction seems to show little spatial variation across mainland China (Fig. 2c). With respect to CLSM LAI error, regions in southern China that have generally higher LAI show larger standard deviation in SPOT LAI time series (Fig. 2d and 2h). The IVd-based estimates of SMAP L4 LE error, which represent a potential control factor for water-balance errors in CLSM, generally show low-level of error across mainland China (Fig. 2e).

For O-F Tb residuals describing RTM-related error, a higher standard deviation of O-F Tb residuals is observed in the North China Plain (Fig. 2f), which is very consistent in spatial distribution with areas displaying the highest and most significant SSM prediction improvement (Fig. 1c). This is expected, as mentioned above, because O-F Tb residuals are the basis for the soil moisture corrections (or increments) that are applied in the DA system as part of the L4 analysis. The 2017-2018 mean of soil roughness and the 2017-2018 mean LAI show higher values in southwest and southeast China (Fig. 2g-h).

https://doi.org/10.5194/hess-2020-407
Preprint. Discussion started: 9 September 2020

Hydrology and Earth System Sciences
Discussions

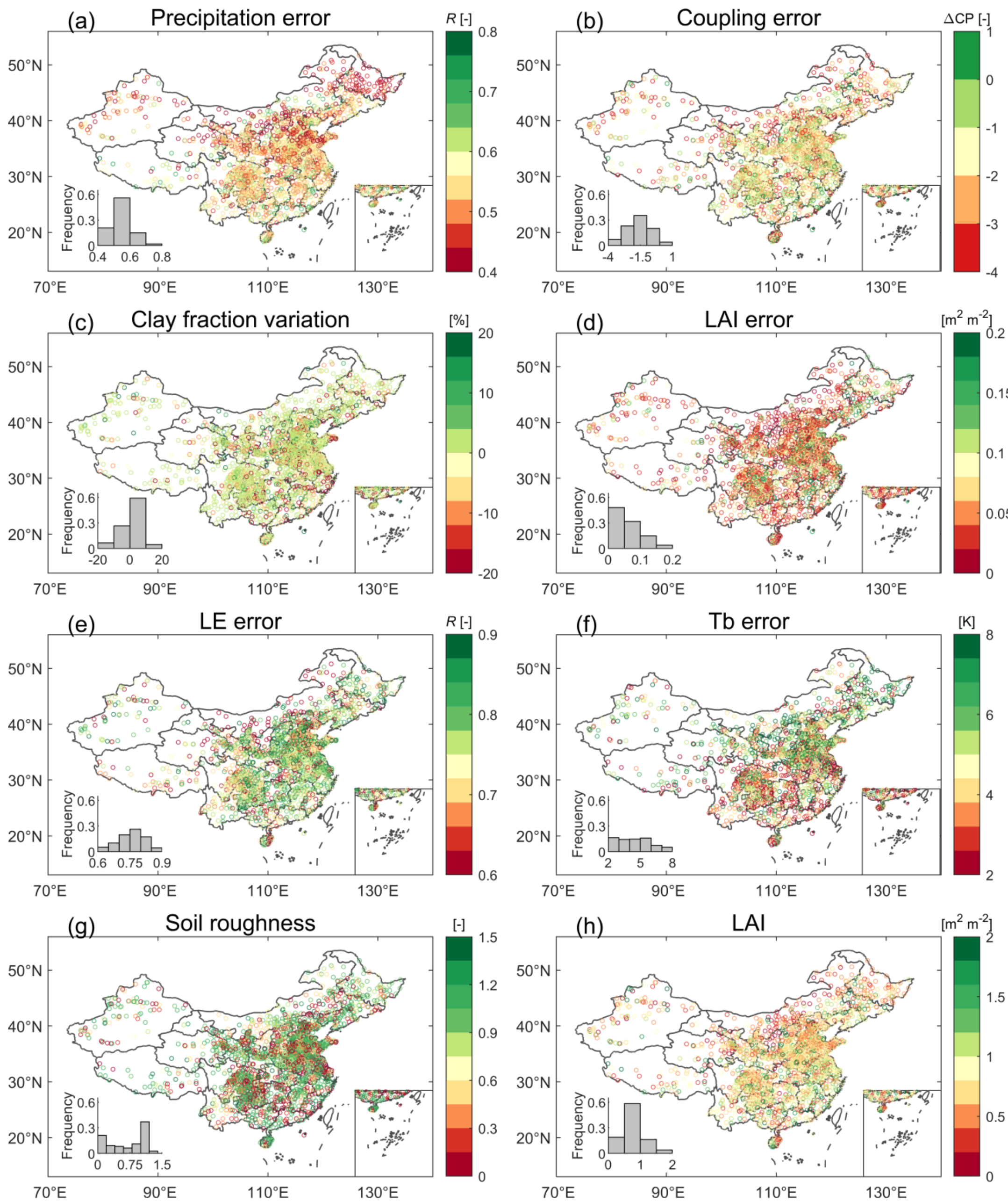

Figure 2: Factors potentially influencing SMAP L4 performance over mainland China: (a) CLSM precipitation error measured by the Spearman's rank correlation between CLSM precipitation and ground observations; (b) SSM-RZSM coupling strength error (CP_{OL} minus CP_{obs}); (c) clay fraction variation (difference) across the soil profile; (d) error in LAI input to L4; (e) IVd-based error of LE from L4; (f) Tb error; (g) L4 microwave soil roughness; (h) climatology mean of LAI input to L4.

https://doi.org/10.5194/hess-2020-407
Preprint. Discussion started: 9 September 2020

Hydrology and Earth System Sciences Discussions

3.3 Attribution of SMAP L4 versus OL performance to control factors

3.3.1 Attribution using random forest regression

As mentioned above, RF regression was used to identify the relative importance of our 8 control factors for determining the efficiency of SMAP L4 DA (i.e., $\Delta R = R_{L4} - R_{OL}$), and also L4 ($R_{L4}$) and OL performances ($R_{OL}$). To start, we first investigate the robustness of RF for predicting ΔR. To estimate the magnitude of randomness in the RF algorithm, we use 50 bootstrap runs. As shown in Fig. 3a, the 10-fold cross-validation test (228 validation samples) shows that the predicted and in-situ-based ΔR have a mean correlation of 0.72 and 0.46 for SSM and RZSM, respectively.

Given the sampling errors of ΔR, which is based on a two-year validation period, and the relatively low spatial variability in RZSM skill (Figs. 1f), the performance of RF is acceptable. In addition, ground-measurement upscaling error is likely a significant contributor to unexplainable spatial variability for ΔR in Fig. 1. In fact, Chen et al. (2016) found large spatial variability in the ability of point-scale SSM ground observations to describe grid cell-scale SSM dynamics. In-situ observations sites associated with larger upscaling errors will introduce a spurious low bias into sampled estimates of ΔR values (see Appendix B in Dong et al., 2020). Therefore, some of the ΔR spatial variability observed in Fig. 1 is unrelated to any aspect of the L4 system and is therefore unexplainable via the 8 control factors we have selected.

https://doi.org/10.5194/hess-2020-407
Preprint. Discussion started: 9 September 2020

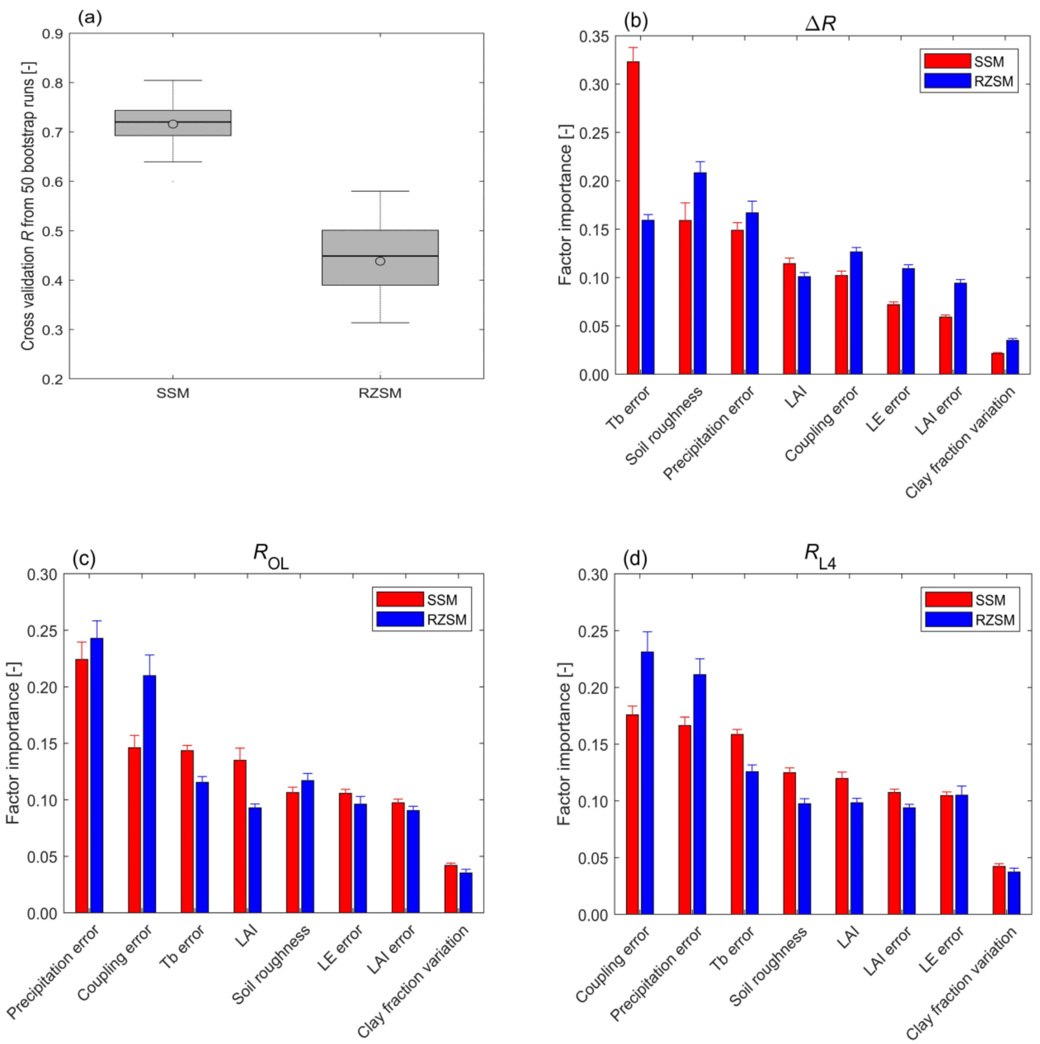

Figure 3: Attribution analysis of SMAP L4 DA efficiency: (a) Cross-validation of RF regression method in predicting DA efficiency $\Delta R = R_{L4} - R_{OL}$ based on our 8 control factors (Table 1). Relative importance of 8 control factors determining spatial patterns in (b) DA efficiency (ΔR), (c) OL performance (R_{OL}), and (d) L4 performance (R_{L4}). Red (blue) bars represent predictor importance for SSM (RZSM). Error bars reflect the standard deviation from 50-member bootstrapping of the RF importance estimates.

Based on the RF results, the Tb error is quantified as the most prominent factor in determining DA efficiency (i.e., $\Delta R = R_{L4} - R_{OL}$) – followed by precipitation error and microwave soil roughness (Fig. 3b). The RF-derived ranking of control-factor importance for RZSM is similar to that of SSM in that the same three factors are still the most explanatory. However, in contrast to SSM, the importance of Tb error for RZSM decreased dramatically from >30% to ~15%. Other modeling error sources (e.g., the vertical variability of soil properties) have only very limited impact on SMAP DA improvement.

As seen in Fig. 3c, for the OL performance (R_{OL}), the most important factors identified by RF include precipitation error, SSM-RZSM coupling error, and Tb error (microwave soil roughness) for SSM (RZSM). Note that although the Tb error is identified as third important factor for R_{OL} in SSM skill, this is an instance where there is correlation (poorer skill happens to coincide with higher Tb error), but this does not imply a causal relationship. Specifically, it is normal that Tb (O-F) errors are higher where the OL performs worse, but a high Tb error is not the cause of a low OL performance. The same applies to the relationship between microwave soil roughness and OL skill for RZSM estimation. The SMAP L4 system is able to reduce the predominant impact of precipitation errors on both SSM and RZSM estimation skill, rendering SSM-RZSM coupling error the most important factor for R_{L4} (Fig. 3d). In addition, in the L4 system, the high vegetation density effect on SSM and RZSM estimation is clearly reduced, as the fourth most important factor of LAI is replaced by Tb error.

The qualitative rankings provided by the RF analysis in Fig. 3 are relatively robust to our particular choice of benchmark data set to define the 'error' of various control variables. For instance, we replaced the CGDPA precipitation benchmark with the CMORPH-merge product (Version 1, last access: 6 April 2020; DOI: https://doi.org/10.25921/w9va-q159; Xie et al., 2019), which is the 0.1 degree merging product of CMORPH and observations from more than 30,000 automatic weather stations in mainland China. For this case, the predictive power of the regression model established by the RF is not affected (similar to Fig. 3a), and the qualitative rankings of the precipitation error in R_{OL} and R_{L4} are not impacted (similar to Fig. 3c-d).

3.3.2 Attribution using box plot comparisons

As stated in Section 2.5, the RF method is adept at summarizing the impact of multiple (co-varying) control factors simultaneously in the established regression model and thus provides more comprehensive insights than the examination of how the target variable (DA improvement) fluctuates with each individual control factor. However, it does not allow the investigation of the sign of the relationship between DA improvement and each control factor – which is important for understanding exactly how each factor influences the DA system. In addition, since the net impact of various factors can enhance DA efficiency by either degrading the OL or enhancing the ability of DA to add more value, it is important to decompose the source of variations in ΔR. Therefore, in addition to examining how SMAP DA efficiency, i.e., $\Delta R = R_{L4} - R_{OL}$, varies as a function of the most prominent control factors identified in the above Section 3.3.1 (i.e., Tb error, precipitation forcing, and microwave soil roughness), we also examine how precipitation error as a control factor affects the OL performance, i.e., R_{OL}.

https://doi.org/10.5194/hess-2020-407
Preprint. Discussion started: 9 September 2020

To minimize the uncertainty caused by large errors in each of the control factors, we exclude samples with errors (separately for each control factor) ranking above the 80th percentile in the following analysis. The relationship between Tb errors and L4 DA efficiency is straightforward: higher Tb errors are associated with higher ΔR, with ΔR generally larger for SSM than for RZSM (Fig. 4a-b).

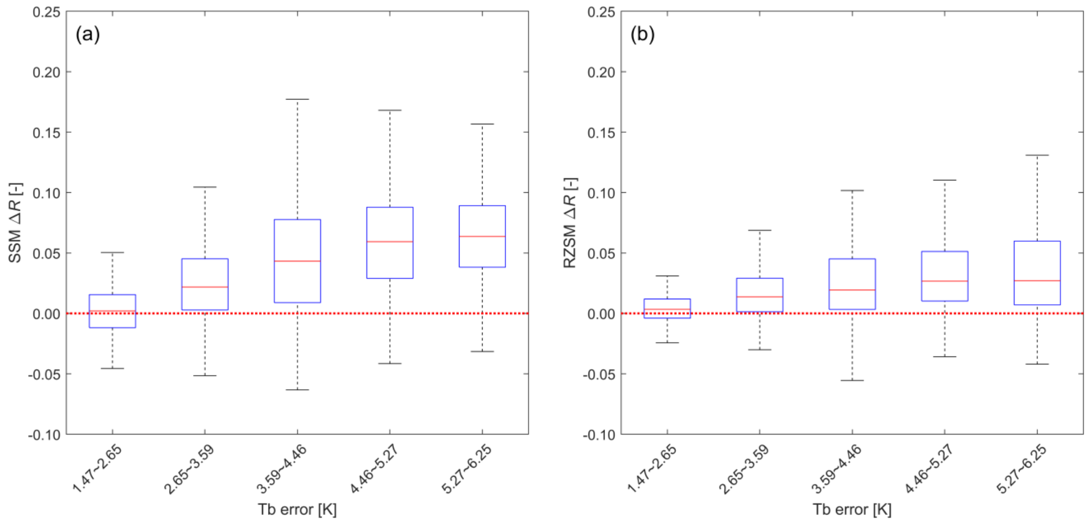

Figure 4: SMAP L4 DA efficiency ($\Delta R = R_{L4} - R_{OL}$) as a function of Tb error for (a) SSM and (b) RZSM. Samples with Tb error ranking above the 80th percentile are excluded from the analysis.

For precipitation, this decomposition is illustrated in Fig. 5. Note that, as expected, low-quality precipitation tends to degrade the skill (i.e., correlation versus ground observations) of OL SSM and RZSM estimates (see Fig. 5a-b). This degradation provides an enhanced opportunity for SMAP L4 DA to provide added value. As a result, ΔR tends to be a proportional function of precipitation skill (i.e., higher precipitation skill leads to lower ΔR, see Fig. 5c-d). This inverse relationship is a well-known tendency for land data assimilation systems (Liu et al., 2011; Bolten and Crow, 2012; Dong et al., 2019a). Precipitation quality has a diminished impact on RZSM estimation skill compared to SSM estimation skill. This is expected since RZSM is (essentially) the result of applying a low-pass time series filter to precipitation. As such, it is less sensitive to high-frequency errors in precipitation products than SSM is.

https://doi.org/10.5194/hess-2020-407
Preprint. Discussion started: 9 September 2020

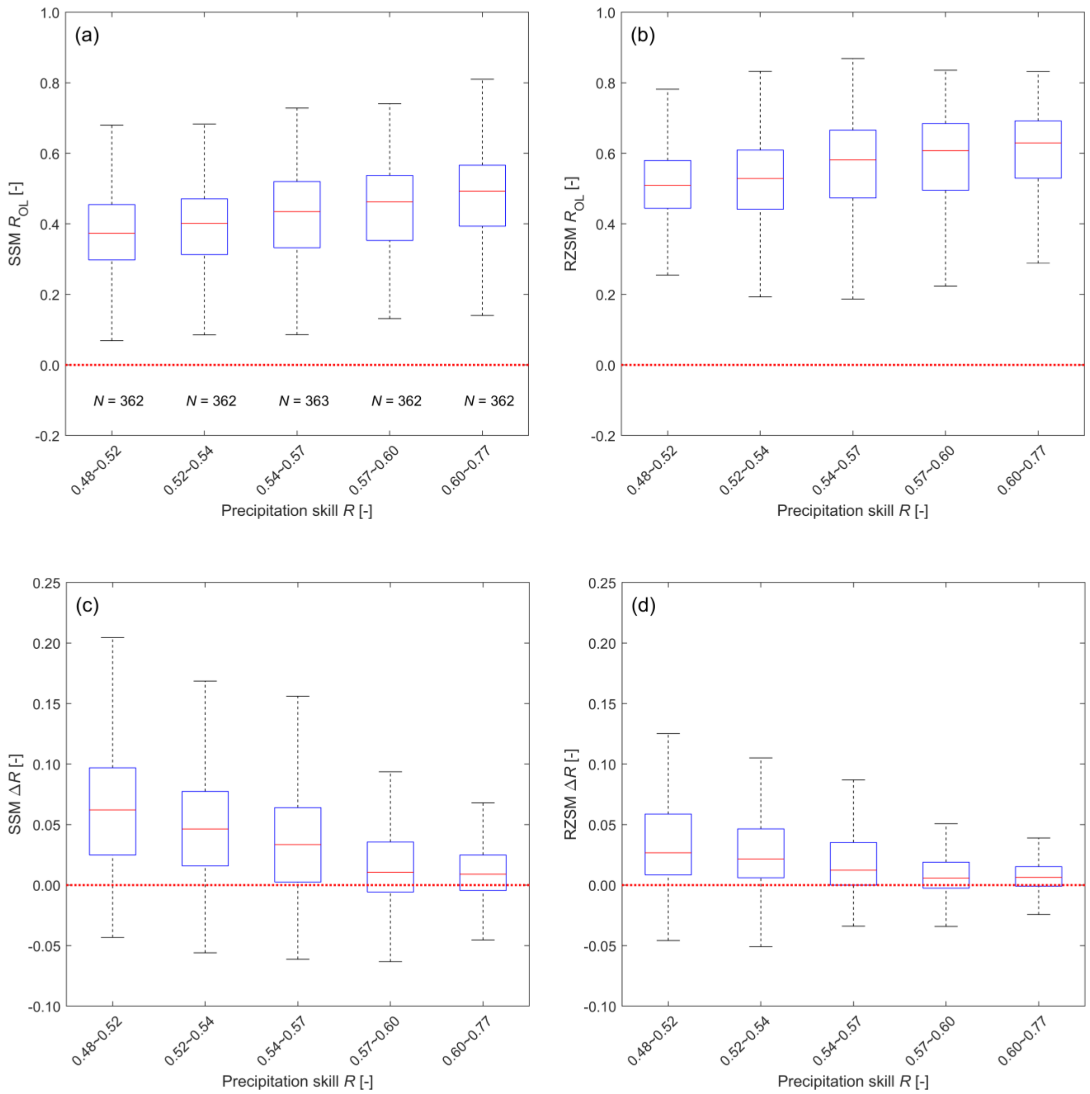

Figure 5: OL performance (R_{OL}) as a function of precipitation forcing skill R for (a) SSM and (b) RZSM. SMAP L4 DA efficiency ($\Delta R = R_{L4} - R_{OL}$) as a function of precipitation skill for (c) SSM and (d) RZSM. Samples with precipitation skill ranking below the 20th percentile are excluded from the analysis.

Figure 6 is analogous to Fig. 4 but shows skill differences ΔR as a function of microwave soil roughness. Similar to Tb errors, it is as expected that this control factor of microwave soil roughness has little impact on the OL performance, except that R_{OL} shows slight decreasing tendency with increasing soil roughness (not shown). Given the fact that the

https://doi.org/10.5194/hess-2020-407
Preprint. Discussion started: 9 September 2020

Hydrology and Earth System Sciences
Open Access
EGU
Discussions

OL does get worse with increasing roughness, there is more room for improvement as the roughness increases, which makes it plausible that ΔR increases with increasing soil roughness (see Fig. 6a-b).

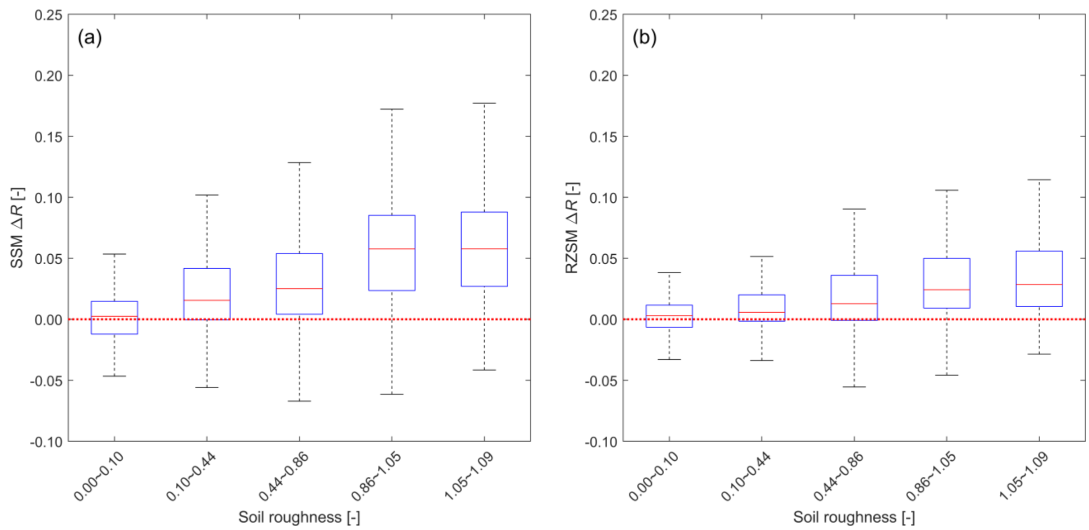

Figure 6: As in Fig. 4 but for ΔR as a function of microwave soil roughness.

Besides the above three control factors that dominate the DA efficiency, we also examine the top factor that affects SMAP L4 performance, i.e., vertical-coupling errors (Fig. 7). As expected, larger (absolute) bias in SSM-RZSM coupling in CLSM tends to be associated with degraded OL estimates of both SSM and RZSM (see Figs. 7a-b), although the analysis does not prove such a causal relationship. Similar to precipitation errors above, decreased OL skill (seen on the left-hand-side of the figures) provides an opportunity for increased DA efficiency – which is clearly seen in Fig. 7. However, such increases are much larger for SSM than for RZSM.

For RZSM, SSM-RZSM coupling bias represents a double-edged sword. While such bias leads to an enhanced opportunity to improve upon a degraded OL, it should also hamper the ability of DA to transfer SSM increments into the root-zone – particularly when, like here, the bias reflects the lack of vertical coupling in the model (Kumar et al., 2009). This means that some of the opportunity presented by the larger OL RZSM errors is squandered by sub-optimal DA. As a result, the increase in RZSM DA efficiency associated with biased SSM-RZSM coupling (Fig. 7d) is smaller than the analogous increase in SSM DA efficiency (Fig. 7c).

https://doi.org/10.5194/hess-2020-407
Preprint. Discussion started: 9 September 2020

Hydrology and Earth System Sciences
Discussions

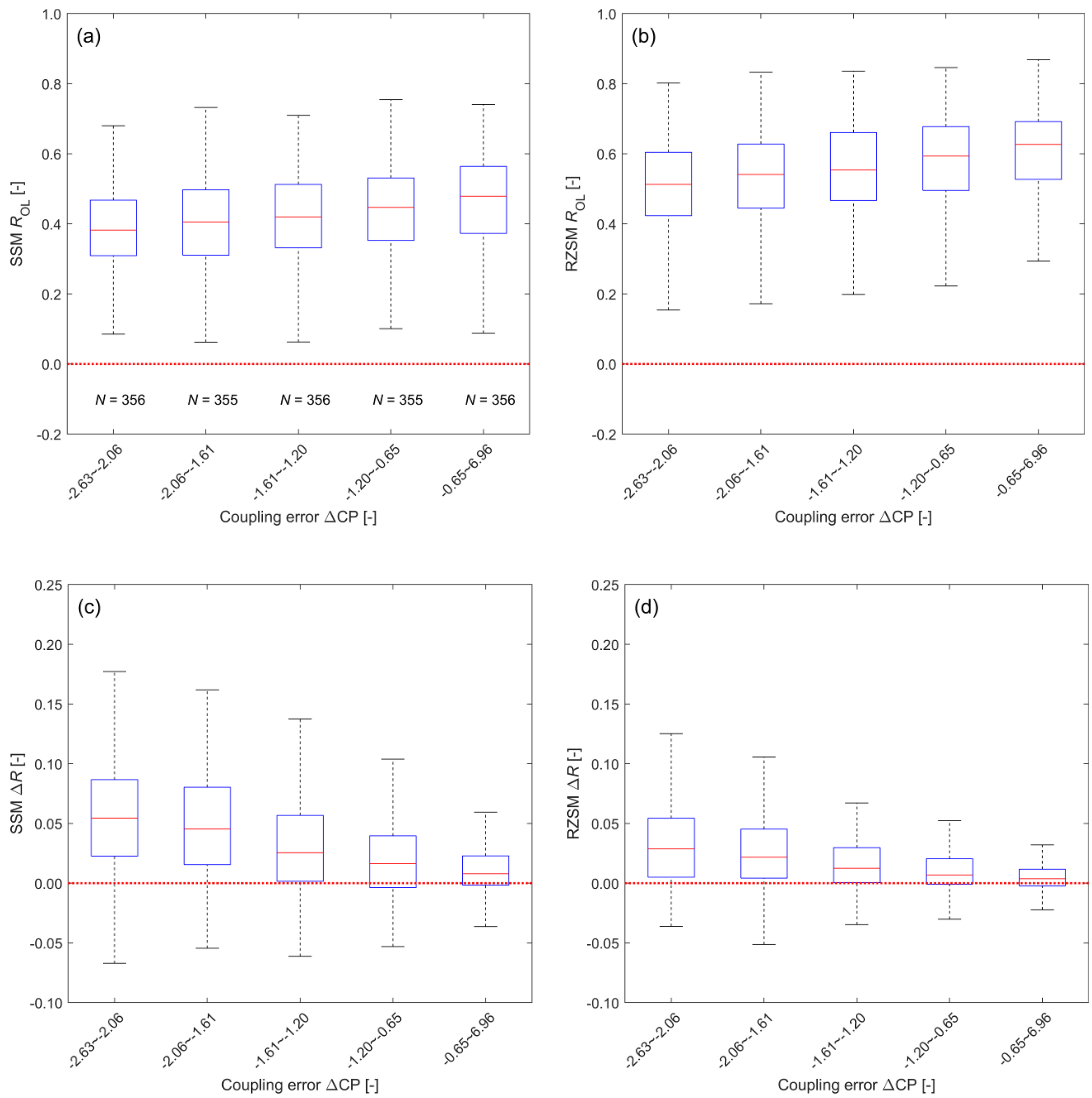

Figure 7: As in Fig. 5 but for R_{OL} and ΔR as a function of SSM-RZSM coupling error indicated by the CP difference ($\Delta CP = CP_{OL} - CP_{obs}$).

For the three strongest control factors that determine DA efficiency ΔR, i.e., Tb error, precipitation error and microwave soil roughness, we further conducted paired one-way analysis of variance (not shown). Results indicates that for each of the five binned groups separated by each of the above-mentioned three control factors, the inter-group difference in ΔR caused by each control factor is significant (p<0.01) for both SSM and RZSM. In addition, except for

https://doi.org/10.5194/hess-2020-407
Preprint. Discussion started: 9 September 2020

Hydrology and Earth System Sciences
Open Access
Discussions

the groups with lowest mean ΔR in Fig. 4a and Fig. 6a, the averages of ΔR from all groups are significantly higher than 0 (p<0.01).

As expected, precipitation error is the dominant factor for explaining the skill of the OL estimates. In contrast, the SSM-RZSM coupling error is the dominant factor for explaining the skill of the L4 results, which shows DA is able to correct for precipitation errors.

4 Conclusions

The SMAP L4 algorithm assimilates L-band Tb observations into the Catchment Land Surface Model, to provide surface and root-zone soil moisture estimates (i.e., SSM, RZSM) with global, 3-hourly coverage at 9-km resolution. The performance of the L4 soil moisture estimates compared to a baseline model-only simulation (OL) is influenced by multiple control factors associated with the land surface modelling (LSM) and radiative transfer modeling (RTM) components of the L4 system. In this study, we assess the performance of SMAP L4 DA system using the 2 years of in-situ soil moisture profile observations at 2474 sites across mainland China. We apply a random forest (RF) regression to identify the dominant factors that control the spatial distribution of the DA efficiency (defined as the skill difference between the L4 and OL estimates of SSM and RZSM as measured by their Spearman rank correlation with in-situ measurements). Results show that L4 improves SSM prediction skill by 14% on average, with over 77% of the 2287 9-km EASE grid cells showing an increase in Spearman's rank correlation with in-situ observations. Similarly widespread but smaller improvements are also observed in RZSM, with averaged R improvement of 7%.

Based on the RF regression analysis, the added value of SMAP L4 DA for SSM is primarily determined by Tb error (measured by standard deviation of O-F Tb residuals), followed by microwave soil roughness and daily precipitation error. These three factors are also the most prominent factors controlling SMAP DA improvement for RZSM, albeit with the Tb error being the least important of these three factors for RZSM DA efficiency.

Generally, the OL performance clearly decreases with increasing precipitation error, whereas for L4 performance precipitation error is not identified as the most dominant control factor. This indicates that the L4 system is able to correct for errors in precipitation forcing. In addition, our results demonstrate that SMAP DA contributes the most added value for cases where CLSM underestimates SSM-RZSM vertical coupling strength. However, due to the difference in top-layer soil depth between the in-situ observations (10 cm) and the L4 analysis (5 cm), it is unclear whether or not the observed SSM-RZSM coupling strength biases are real in an absolute sense – or simply reflect inconsistencies in the depth of modelled versus observed SSM and RZSM time series. Nevertheless, it is worth stressing that, despite the ambiguity with regards to their absolute magnitude/sign, relative variations in apparent SSM-RZSM coupling biases explain a significant amount of the observed spatial variation in L4 performance. Therefore, this finding clearly underpins the importance of properly specifying SSM-RZSM coupling strength in CLSM as a way to improve the SMAP L4 product.

For SMAP L4 SSM skill, the next-most important factors (after SSM-RZSM coupling) are the precipitation error, the Tb error and microwave soil roughness (Fig. 3d). For L4 RZSM skill, the next-most important factors (after SSM-RZSM coupling) are the precipitation error, the Tb error and the LE error, with the latter two factors of comparable importance (Fig. 3d). To enhance the L4 performance, additional focus should thus be placed on improving the model's characterization of the partitioning of the available energy into latent and sensible heat (LE error) and the microwave radiative transfer modeling (Tb error).

Data availability

The SMAP L4 datasets are available from https://nsidc.org/data/SPL4SMAU/versions/4. Gauge-based precipitation dataset CGDPA is from http://data.cma.cn/data/cdcdetail/dataCode/SEVP_CLI_CHN_PRE_DAY_GRID_0.25.html. The availabilities of other datasets are stated in their corresponding subsections.

Author contributions

Jianxiu Qiu and Jianzhi Dong conceptualized the study. Jianxiu Qiu carried out the analysis and wrote the first draft manuscript, Wade Crow refined the work, Jianzhi Dong, Rolf Reichle, and Gabrielle De Lannoy helped with the analysis. All authors contributed to the analysis, interpretation of the results and writing.

Competing interests

The authors declare that they have no conflict of interest.

Acknowledgments

This work was supported by National Natural Science Foundation of China (Grant Nos. 41971031, 41501450). Rolf Reichle was supported by the NASA SMAP mission. Gabrielle De Lannoy was supported by KU Leuven C1 (C14/16/045). The findings, conclusions and representations of fact in this publication are those of the authors and should not be construed to represent any official USDA or U.S. Government determination or policy.

References

Baret, F., Weiss, M., Lacaze, R., Camacho, F., Makhmara, H., Pacholcyzk, P., and Smets, B.: GEOV1: LAI, FAPAR Essential Climate Variables and FCOVER global time series capitalizing over existing products. Part1: Principles of development and production, Remote Sens. Environ., 137, 299-309, doi:10.1016/j.rse.2013.02.030, 2013.

Bolten, J.D. and Crow, W.T.,: Improved prediction of quasi-global vegetation conditions using remotely-sensed surface soil moisture, Geophys. Res. Lett., 39(19), doi:10.1029/2012GL053470, 2012.

Breiman, L.: Random forests, Mach. Learn., 45(1), 5–32, doi:10.1023/A:1010933404324, 2001.

Chan, S., Njoku, E. G. and Colliander A.: SMAP L1C radiometer half-orbit 36 km EASE-Grid brightness temperatures, version 3. NASA National Snow and Ice Data Center Distributed Active Archive Center, 10.5067/E51BSP6V3KP7, 2016.

Chen, F., Crow, W.T., Starks, P.J. and Moriasi, D.N.: Improving hydrologic predictions of a catchment model via assimilation of surface soil moisture, Adv. Water Resources., 34(4), 526-536, doi:10.1016/j.advwatres.2011.01.011, 2011.

Chen, F., Crow, W.T., Colliander, A., Cosh, M.H., Jackson, T.J., Bindlish, R., Reichle, R.H., Chan, S.K., Bosch, D.D., Starks, P.J., and Goodrich, D.C.: Application of triple collocation in ground-based validation of Soil Moisture Active/Passive (SMAP) level 2 data products, IEEE JSTARS., 99, 1-14, doi:10.1109/JSTARS.2016.2569998, 2016.

Crow, W.T. and Van Loon, E.: The impact of incorrect model error assumptions on the sequential assimilation of remotely sensed surface soil moisture, J. Hydrometeorol., 8(3), 421-431, doi:10.1175/jhm499.1, 2006.

De Lannoy, G. J. M., Reichle, R. H., and Pauwels, V. R. N.: Global calibration of the GEOS-5 L-band microwave radiative transfer model over nonfrozen land using SMOS observations, J. Hydrometeorol., 14(3), 765–785, doi:10.1175/JHM-D-12-092.1, 2013.

De Lannoy, G. J. M., Reichle, R. H., and Vrugt, J. A.: Uncertainty quantification of GEOS-5 L-band radiative transfer model parameters using Bayesian inference and SMOS observations, Remote Sens. Environ., 148, 146–157, doi :10.1016/j.rse.2014.03.030, 2014.

Dong, J., Crow, W.T., Reichle, R., Liu, Q., Lei, F., and Cosh, M.: A global assessment of added value in the SMAP Level 4 soil moisture product relative to its baseline land surface model, Geophys. Res. Lett., 46, 6604-6613, doi:10.1029/2019GL083398, 2019a.

Dong, J., Crow, W.T., Duan, Z., Wei, L., and Lu, Y.: A double instrumental variable method for geophysical product error estimation, Remote Sens. Environ., 225, 217-228, doi:10.1016/j.rse.2019.03.003, 2019b.

Dong, J., Crow, W.T., Tobin, J. K., Cosh, H. M., Bosch, D. D., Starks, J. P., Seyfried, M., and Collins, H. C.: Comparison of microwave remote sensing and land surface modeling in surface soil moisture climatology estimation, Remote Sens. Environ., 242, 111756, doi :10.1016/j.rse.2020.111756, 2020.

Entekhabi, D., Njoku, E. G., O'Neill, P. E., Kellogg, K. H., Crow, W. T., and Edelstein, W. N.: The soil moisture active passive (SMAP) mission, P. IEEE., 98(5), 704–716, doi:10.1109/jproc.2010.2043918, 2010.

Gruber, A., De Lannoy, G., Albergel, C., Al-Yaari, A., Brocca, L., Calvet, J. C., and Draper, C.: Validation practices for satellite soil moisture retrievals: What are (the) errors?, Remote Sens. Environ., 244, 111806, doi:10.1016/j.rse.2020.111806, 2020.

Gupta, H. V., Kling, H., Yilmaz, K. K., and Martinez, G. F.: Decomposition of the mean squared error and NSE performance criteria: Implications for improving hydrological modelling, J. Hydrometeorol., 377(1-2), 80-91, doi:10.1016/j.jhydrol.2009.08.003, 2009.

Jung, M., Koirala, S., Weber, U., Ichii, K., Gans, F., Camps-Valls, G., and Reichstein, M.: The FLUXCOM ensemble of global land-atmosphere energy fluxes, Sci. Data., 6(1), 1-14, doi:10.1038/s41597-019-0076-8, 2019.

Kumar, S.V., Reichle, R.H., Koster, R.D., Crow, W.T., and Peters-Lidard, C.D.: Role of subsurface physics in the assimilation of surface soil moisture observations, J. Hydrometeorol., 10, 1534-1547, doi:10.1175/2009JHM1134.1, 2009.

Lucchesi, R.: File specification for GEOS-5 FP, NASA GMAO Office Note 4 (version 1.0), 63 pp. Available at https://ntrs.nasa.gov, 2013

McColl, K., Vogelzang, J., Konings, A.G., Entekhabi, D., Piles, M., and Stoffelen, A.: Extended triple collocation: Estimating errors and correlation coefficients with respect to an unknown target, Geophys. Res. Lett., 41(17), 6229-6236, doi:10.1002/2014gl061322, 2014.

Piepmeier, J. R., Focardi, P., Horgan, K. A., Knuble, J., Ehsan, N., Lucey, J., Brambora, C., Brown, P. R., Hoffman, P. J., French, R. T., Mikhaylov, R. L., Kwack, E. Y., Slimko, E. M., Dawson, D. E., Hudson, D., Peng, J., Mohammed, P. N., de Amici, G., Freedman, A. P., Medeiros, J., Sacks, F., Estep, R., Spencer, M. W., Chen, C. W., Wheeler, K. B., Edelstein, W. N., O'Neill, P. E., and Njoku, E. G.: SMAP L-band microwave radiometer: Instrument design and first year on orbit, IEEE T. Geosci. Remote., 55(4), 1954–1966, doi:10.1109/TGRS.2016.2631978, 2017.

Liu, Q., Reichle, R., Bindlish, R., Cosh, M.H., Crow, W.T., de Jeu, R., de Lannoy, G., Huffman, G.J. and Jackson, T.J.: The contributions of precipitation and soil moisture observations to the skill of soil moisture estimates in a land data assimilation system, J. Hydrometeorol., 12(5), 750-765, doi:10.1175/JHM-D-10-05000.1, 2011.

Reichle, R.H., Crow, W.T., Koster, R. D., Sharif, H. and Mahanama, S.: Contribution of soil moisture retrievals to land data assimilation products, Geophys. Res. Lett., 35(1), doi:10.1029/2007GL031986, 2008.

Reichle, R. H., de Lannoy, G. J. M., Liu, Q., Ardizzone, J. V., Colliander, A., Conaty, A., Crow, W., Jackson, T. J., Jones, L. A., Kimball, J. S., Koster, R. D., Mahanama, S. P., Smith, E. B., Berg, A., Bircher, S., Bosch, D., Caldwell, T. G., Cosh, M., González-Zamora, Á., Holifield Collins, C. D., Jensen, K. H., Livingston, S., Lopez-Baeza, E., Martínez-Fernández, J., McNairn, H., Moghaddam, M., Pacheco, A., Pellarin, T., Prueger, J., Rowlandson, T., Seyfried, M., Starks, P., Su, Z., Thibeault, M., van der Velde, R., Walker, J., Wu, X., and Zeng, Y.: Assessment of the SMAP Level-4 surface and root-zone soil moisture product using in situ measurements, J. Hydrometeorol., 18(10), 2621–2645, doi:10.1175/JHM-D-17-0063.1, 2017a.

Reichle, R. H., de Lannoy, G. J. M., Liu, Q., Koster, R. D., Kimball, J. S., Crow, W. T., Ardizzone, J. V., Chakraborty, P., Collins, D. W., Conaty, A. L., Girotto, M., Jones, L. A., Kolassa, J., Lievens, H., Lucchesi, R. A., and Smith, E. B.: Global assessment of the SMAP Level-4 surface and root-zone soil moisture product using assimilation diagnostics, J. Hydrometeorol., 18(12), 3217–3237, doi:10.1175/jhm-d-17-0130.1, 2017b.

Reichle, R. H., de Lannoy, G., Koster, R. D., Crow, W. T., Kimball, J. S., and Liu, Q.: SMAP L4 Global 9 km EASE-grid surface and root zone soil moisture land model constants, Version 4, NASA National Snow and Ice Data Center DAAC, https://doi.org/10.5067/KGLC3UH4TMAQ, 2018a

Reichle, R. H., de Lannoy, G., Koster, R. D., Crow, W. T., Kimball, J. S., & Liu, Q.: SMAP L4 global 3-hourly 9 km EASE-grid surface and root zone soil moisture analysis update data, version 4, NASA National Snow and Ice Data Center DAAC, https://doi.org/10.5067/60HB8VIP2T8W, 2018b

Reichle, R. H., de Lannoy, G., Koster, R. D., Crow, W. T., Kimball, J. S., & Liu, Q.: SMAP L4 global 3-hourly 9 km EASE-grid surface and root zone soil moisture geophysical data, version 4, NASA National Snow and Ice Data Center DAAC, https://doi.org/10.5067/KPJNN2GI1DQR, 2018c

Reichle, R. H., Liu, Q., Koster, R. D., Crow, W. T., De Lannoy, G. J., Kimball, J. S., and Kolassa, J.: Version 4 of the SMAP Level-4 soil moisture algorithm and data product, J. Adv. Model Earth Sy., 11(10), 3106-3130, doi:10.1029/2019MS001729, 2019.

Seneviratne, S. I., Corti, T., Davin, E. L., Hirschi, M., Jaeger, E. B., and Lehner, I.: Investigating soil moisture–climate interactions in a changing climate: A review, Earth-Sci. Rev., 99, 125–161, doi:10.1016/j.earscirev.2010.02.004, 2010.

Seneviratne, S. I., Wilhelm, M., Stanelle, T., Hurk, B., Hagemann, S., and Berg, A.: Impact of soil moisture-climate feedbacks on CMIP5 projections: First results from the GLACECMIP5 experiment, Geophys. Res. Lett., 40(19), 5212-5217, doi:10.1002/grl.50956, 2013.

https://doi.org/10.5194/hess-2020-407
Preprint. Discussion started: 9 September 2020

Hydrology and Earth System Sciences Discussions

Shen, Y., Xiong, A., Wang, Y., and Xie, P.: Performance of high-resolution satellite precipitation products over China, J. Geophys. Res-Atmos., 115(D2), doi:10.1029/2009JD012097, 2010.

Shen, Y. and Xiong, A.: Validation and comparison of a new gauge-based precipitation analysis over mainland China, Int. J. Climatol., 36(1), 252-265, doi:10.1002/JOC.4341, 2015.

Verger, A., Baret, F., and Weiss, M.: Performances of neural networks for deriving LAI estimates from existing CYCLOPES and MODIS products, Remote Sens. Environ., 112, 2789-2803, doi:10.1016/j.rse.2008.01.006, 2008.

Xie, P., Yatagai, A., Chen, M., Hayasaka, T., Fukushima, Y., Liu, C., and Yang, S.: A gauge-based analysis of daily precipitation over East Asia, J. Hydrometeorol., 8, 607-626, doi:10.1175/JHM583.1, 2007.

Xie, P., Joyce, R., Wu, S., Yoo, S.-H., Yarosh, Y., Sun, F., Lin, R..: NOAA CDR Program: NOAA Climate Data Record (CDR) of CPC Morphing Technique (CMORPH) High Resolution Global Precipitation Estimates, Version 1. NOAA National Centers for Environmental Information, 2019.